PERGAMON

Journal of Geodynamics 35 (2003) 391–414

JOURNAL OF
GEODYNAMICS

www.elsevier.com/locate/jog

Recent crustal movements observed with the European VLBI network: geodetic analysis and results

R. Haas[a,*], A. Nothnagel[b], J. Campbell[b], E. Gueguen[c]

[a]*Onsala Space Observatory, Chalmers University of Technology, SE-439 92 Onsala, Sweden*
[b]*Geodätisches Institut der Universität Bonn, Nußallee 17, DE-53 115 Bonn, Germany*
[c]*Istituto di Technologia Informatica Spaziale, Consiglio Nazionale delle Ricerche, IT-75100 Matera, Italy*

Abstract

Purely European geodetic Very Long Baseline Interferometry (VLBI) has been performed at regular intervals since January 1990. Meanwhile 10 VLBI sites in Europe from Sicily to Spitzbergen and the Iberian pensinsula to the Crimean peninsula contribute to the observation series. The observations are used to determine recent crustal movements in these parts of Europe. Baseline measurements are achieved with an accuracy of 2.0 mm plus an additional term depending on the baseline length of less than 1 part-per-billion. Significant horizontal crustal movements are determined with relative accuracies in the range of 10–40%, significant vertical crustal movements are determined with relative accuracies in the range of 30–40%. The determined crustal movements form thus a sound basis for interpretations in a geophysical and geological context. This article concentrates on a description of the geodetic VLBI data analysis, the analysis models used and the results for crustal movements.

1. Introduction

The European geodetic Very Long Baseline Interferometry (VLBI) programme was started in January 1990. The objectives of the observation series are to determine crustal motion in Europe and to provide a stable reference frame for other space geodetic techniques used in the area. The observation sessions are optimised for these goals and involve European radio telescopes only on a regular basis of about six observation sessions per year.

The network configuration evolved from a concentration of radio telescopes in central and southern Europe in the early years to today's coverage of an area extending north–south from Spitzbergen to Sicily and west–east from the Iberian peninsula to the Crimean peninsula. Thus, the network area covers several geophysically interesting regions in Europe, i.e. the Fennoscan-

* Corresponding author. Tel.: +46-31-772-5530; fax: +46-31-772-5590.
E-mail address: haas@oso.chalmers.se (R. Haas).

0264-3707/03/$ - see front matter © 2003 Elsevier Science Ltd. All rights reserved.
doi:10.1016/S0264-3707(03)00003-6

dian region, which is affected by glacial isostastic adjustment processes, and the western Mediterranean region, which is affected by the evolution of the Maghrebides-Apennines system (Gueguen et al., 1998).

The project received support by the European Commission in two stages through the European programmes 'Science' and 'Training and mobility of researchers'. The first phase of the project concentrated on the determination of horizontal crustal movements while the second phase focussed on vertical crustal motion. More details on the project, its organisation and management can be found in Campbell (1995, 1996, 1997).

First result for crustal movement from European VLBI based on only a short observation period in the early 1990s have been published by Ward (1994). Campbell and Nothnagel (2000) and Haas et al. (2000) presented crustal motion results based on analysis of longer data series up to the late 1990s. In this article we present results based on the analysis of data of 12 years of observations in the European geodetic VLBI network covering January 1990 to the end of December 2001.

2. Data modeling and data analysis

The analysis of the VLBI data is performed using the Calc/Solve VLBI analysis software package (Ma et al., 1990). Based on the standard software, several improvements regarding different aspects are incorporated in the analysis. Especially the modeling of the solid earth tides and ocean loading are modified with respect to the standard software, and additionally atmospheric loading and thermal deformation effects for the VLBI telescopes are included. Also the handling of constraints for estimation of piece-wise linear atmospheric parameters is modified with respect to the standard software.

The results for crustal movements are derived in a so-called 'two-step analysis approach' (Haas and Nothnagel, 1999; Haas et al., 2000). This analysis procedure is similar to approaches usually used in the analysis of observations performed with permanent Global Positioning System (GPS) networks.

In a first step a so-called 'baseline-solution' is performed, i.e. relative station coordinates for all stations are determined with respect to a reference station in the network. Usually the reference station is modelled moving according to the plate motion model NNR-Nuvel-1A (De Mets et al., 1994) but it could also be some other plate motion model or velocity field. The results are time series of geocentric station coordinates for each station except the reference station but also the full covariance matrices for each observing session. In order to create a European plate fixed frame, the plate motion of the model in the first step, e.g. NNR-Nuvel-1A, is subtracted from the time series of geocentric coordinates (Table 1).

The geocentric Cartesian station coordinates are then transformed into geocentric ellipsoidal ones applying a conventional transformation procedure using the parameters of the WGS84/GRS80 ellipsoid. Also the full covariance matrix between all station coordinates of the solution, i.e. between the three dimensional coordinates of each individual station and between the coordinates of all participating stations, is transformed into the ellipsoidal system. The results of the transformations are ellipsoidal station coordinates for each participating station in the session and the covariance matrix between the ellipsoidal coordinates of all stations in the specific session.

Table 1
Stations of the European geodetic VLBI network with longitude λ, latitude ϕ, telescope diameter d, date of first participation in the European VLBI observation series (date-1), and number of European VLBI observation sessions participated in so far (num)

Station	λ	ϕ	d (m)	date-1	num
Effelsberg	6° 53′ 1″ E	50° 31′ 25″ N	100.0	01.12.1991	14
Madrid	−4° 15′ 0″ E	40° 25′ 42″ N	34.0	26.01.1990	43
Matera	16° 42′ 14″ E	40° 38′ 58″ N	20.0	05.09.1990	50
Medicina	11° 38′ 49″ E	44° 31′ 15″ N	32.0	26.01.1990	49
Noto	14° 59′ 21″ E	36° 52′ 34″ N	32.0	26.01.1990	43
Ny-Ålesund	11° 51′ 54″ E	78° 55′ 47″ N	20.0	26.10.1994	34
Onsala	11° 55′ 32″ E	57° 23′ 43″ N	20.0	26.01.1990	54
Simeiz	30° 15′ 59″ E	44° 24′ 12″ N	22.0	31.08.1994	20
Wettzell	12° 52′ 39″ E	49° 8′ 43″ N	20.0	26.01.1990	58
Yebes	−3° 5′ 22″ E	40° 31′ 27″ N	13.7	08.06.1995	15

In the second step the series of station latitude, longitude and ellipsoidal height are used to determine the topocentric station drifts. In order to express the motions of the stations in millimetres per year, a mean value for longitude, latitude and height for each station is subtracted and the angular positions are transformed into metric north and east components. Finally, least-squares adjustments are performed to estimate offsets and rates of linear regressions for each station, and in some cases also annual periodic signals are estimated. Again the whole covariance information for each session is applied, so e.g. the rate for the height component depends on the results for the east and north components according to the covariance matrix, too.

Some of the European stations suffered from abrupt changes in the station position due to necessary track and wheel repairs. Thus, additional discontinuities in the linear trends are introduced at these epochs. In these cases the same linear rate before and after the discontinuity are estimated but two different offset values, one before and one after the modification, are determined from the least-squares adjustments.

2.1. Reference station and earth orientation

Since VLBI is a differential technique and the extragalactic radio sources observed are at effectively infinitive distance from the earth (Sovers et al., 1998), the coordinates of a reference station have to be fixed in the adjustment. The reference station in the European geodetic VLBI network is chosen to be Wettzell which shows a stable and reliable behaviour from the analysis of international VLBI sessions (Ma and Ryan, 1998). Additionally, the earth rotation parameters (pole coordinates and UT1) have to be introduced as a priori information in order to permit the estimation of station coordinates at all epochs. Therefore, we introduce the C04 series of earth rotation parameters published by the International Earth Rotation Service (IERS C04, 2000). Precession is modelled following the IAU 1976 precession model (Lieske et al., 1977) and nutation offsets are estimated for each VLBI session with respect to the IAU 1980 theory of nutation (Seidelmann, 1982) which is used as a priori.

2.2. Solid earth tides

The modeling of solid earth tides in the data analysis is modified and improved with respect to the standard software and the recommendations of the IERS Conventions (McCarthy, 1996). An harmonic approach is used based on the expansion of the tide generating potential by Tamura (1997) and the frequency and latitude dependent Love and Shida numbers by Wahr (1981). The free-core-nutation (FCN) resonance period is set to 430 sidereal days. The usage of this harmonic solid earth tide model yields a considerable reduction in chi-square of the post-fit residuals compared to the standard software.

2.3. Ocean tide loading

The next order periodic site deformation effect are ocean loading tides. The effects can be predicted based on ocean tide charts, earth structure and corresponding Green's functions (Scherneck, 1991; Farrel, 1972). An automated internet service to calculate ocean tide loading parameters has been developed by Scherneck and Bos (2001) that allows the calculation of ocean tide loading parameters on the basis of 11 different ocean tide models. This automated ocean loading provider is used to model ocean tide loading parameters for the European geodetic VLBI sites. The ocean tide loading models are based on the ocean tide models: (1) SCHW80 (Schwiderski, 1980), (2) FES94.1 (Le Provost et al., 1994), (3) FES95.2 (Le Provost et al., 1998), (4) FES98 (Lefèvre et al., 2000), (5) FES99 (Lefèvre et al., 2000), (6) CSR3.0 (Eanes and Bettadpur, 1995), (7) CSR4.0 (Eanes and Bettadpur, 1995), (8) GOT99.2 (Ray, 1999), (9) GOT00.2 (Ray, 1999), (10) NAO99.b (Matsumoto et al., 2000), and (11) TPXO5 (Egbert et al., 1994). For each of the VLBI sites time series of loading effects are determined for January 1990 to the end of December 2001 with updates of 30 minutes using the 11 different models. Figs. 1–9 show the maximum differences in the time domain for the VLBI stations. It is clearly visible that the differences in the time domain can reach 1–2 mm for the horizontal components but several mm for the vertical component. For example at the site Ny-Ålesund the maximum difference for the vertical component is on the level of 10 mm when comparing the ocean tide loading using the

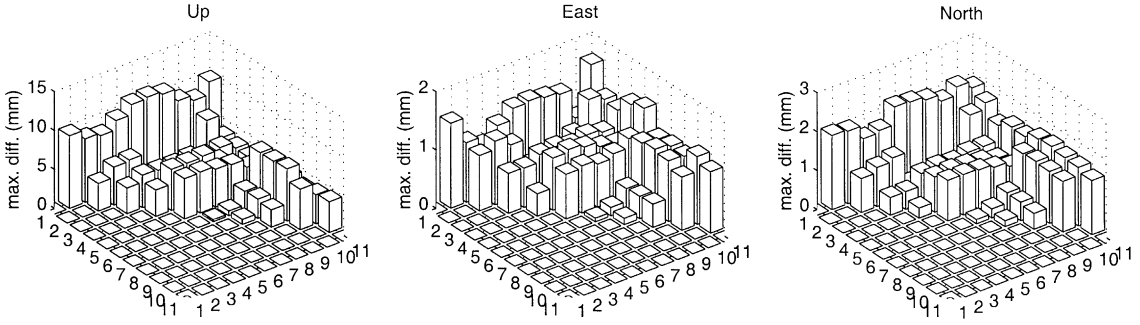

Fig. 1. Maximum differences between time series of ocean loading effects for the site Ny-Ålesund calculated from 11 different ocean tide loading models for January 1990 to end of December 2001 with updates every 30 min. The different ocean loading models are based on the following ocean tide models: (1) SCHW80, (2) FES94.1, (3) FES95.2, (4) FES98, (5) FES99, (6) CSR3.0, (7) CSR4.0, (8) GOT99.2, (9) GOT00.2, (10) NAO99.b, and (11) TPXO5.

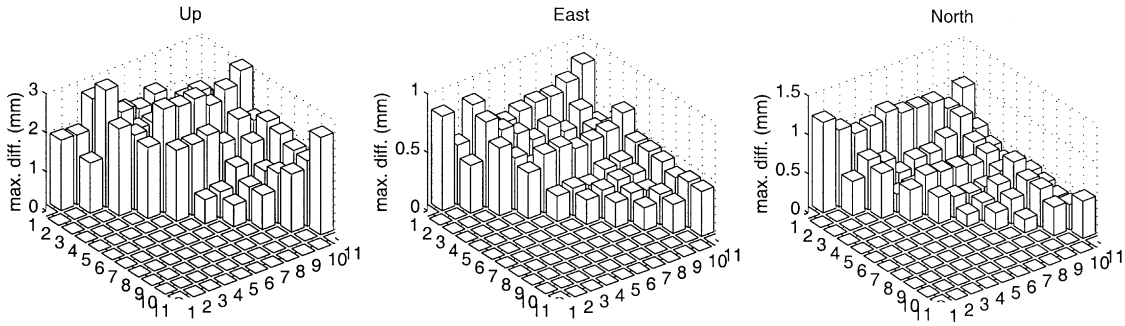

Fig. 2. Maximum differences between time series of ocean loading effects for the site Onsala. For explanation see caption of Fig. 1.

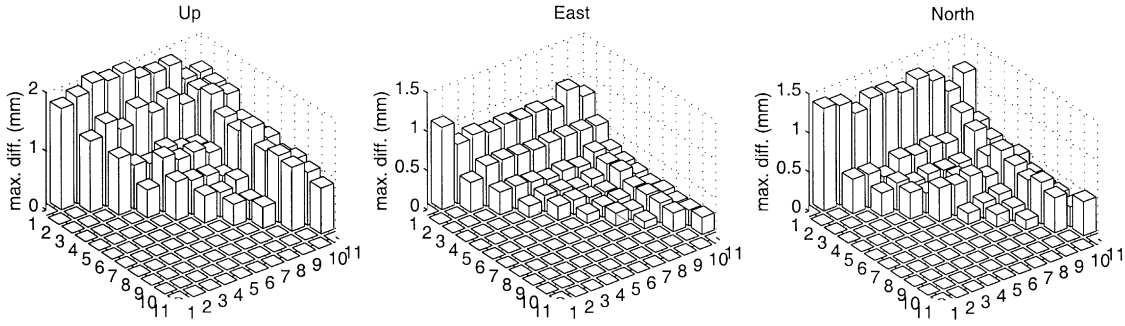

Fig. 3. Maximum differences between time series of ocean loading effects for the site Effelsberg. For explanation see caption of Fig. 1.

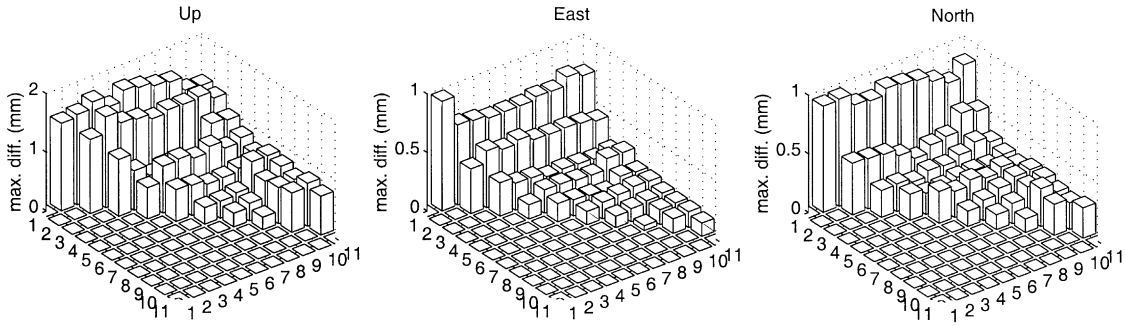

Fig. 4. Maximum differences between time series of ocean loading effects for the site Wettzell. For explanation see caption of Fig. 1.

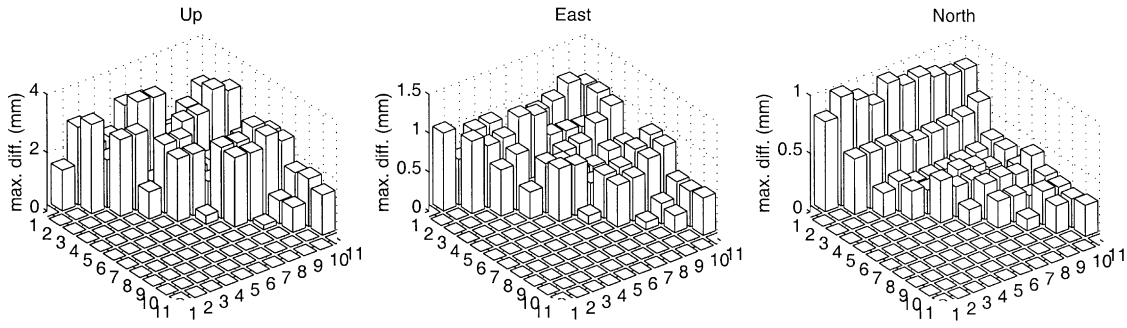

Fig. 5. Maximum differences between time series of ocean loading effects for the site Medicina. For explanation see caption of Fig. 1.

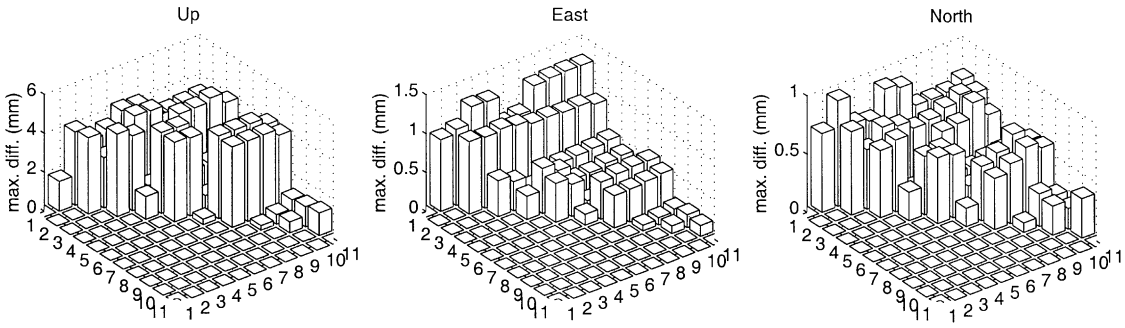

Fig. 6. Maximum differences between time series of ocean loading effects for the site Matera. For explanation see caption of Fig. 1.

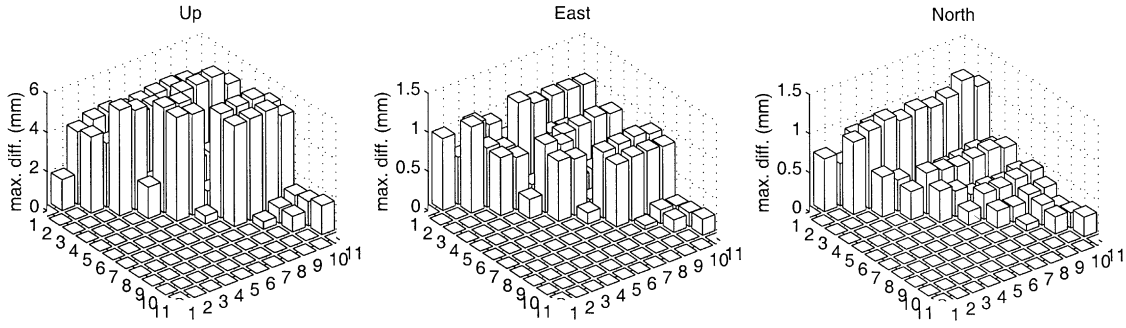

Fig. 7. Maximum differences between time series of ocean loading effects for the site Noto. For explanation see caption of Fig. 1.

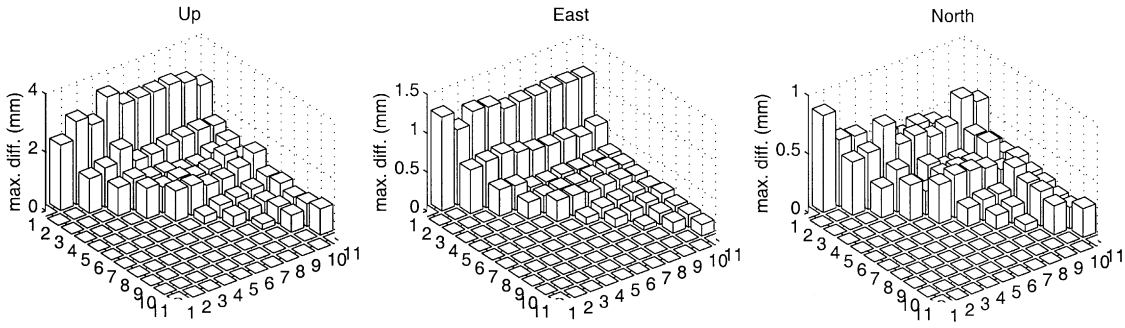

Fig. 8. Maximum differences between time series of ocean loading effects for the site Madrid. For explanation see caption of Fig. 1.

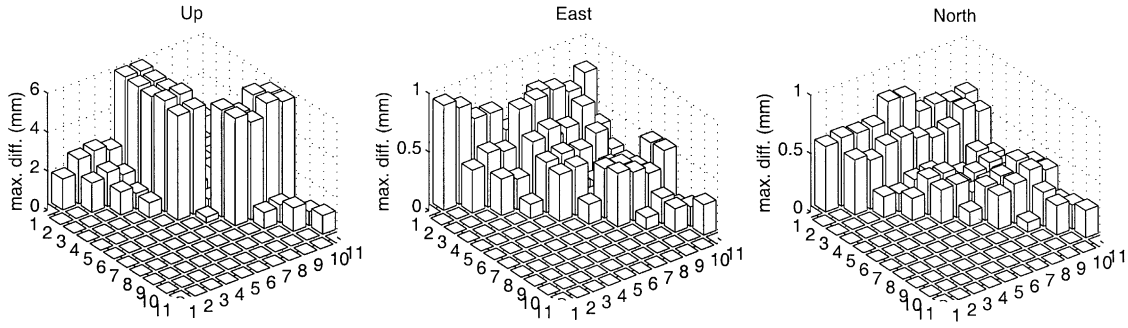

Fig. 9. Maximum differences between time series of ocean loading effects for the site Simeiz. For explanation see caption of Fig. 1.

ocean tide model by Schwiderski (1980) to any of the more recent ocean tide models. Fig. 10 shows the relative reduction of the chi-square of the post-fit residuals with respect to a reference solution using ocean loading based on the ocean tide model by Schwiderski (1980). The reductions are small on the level of 0.1%, but they indicate a slight improvement due to the usage of the more recent ocean tide loading models. For the results on crustal movement presented later, ocean tide loading based on the GOT99.2 ocean tide model is used.

2.4. Atmospheric loading

Changing atmospheric pressure acts as an additional loading effect. The effects can be modelled by convolution of global pressure data and corresponding loading Green's functions. A large data set of modeled atmospheric loading effects has been calculated by Hans-Georg Scherneck and is available on the web-page of the Onsala Space Observatory for all European geodetic VLBI sessions (http://www.oso.chalmers.se/~hgs/apload.html). The computation technique is convolution of global surface pressure fields using Farrell's eastic Green's functions on a spherical earth. As examples, Figs. 11–13 show the modeled topocentric effects on the VLBI reference points at Onsala, Wettzell and Medicina for the time period January 1990 to the end of December 2001. Horizontal displacements due to atmospheric loading amount to 1–2 mm, the vertical

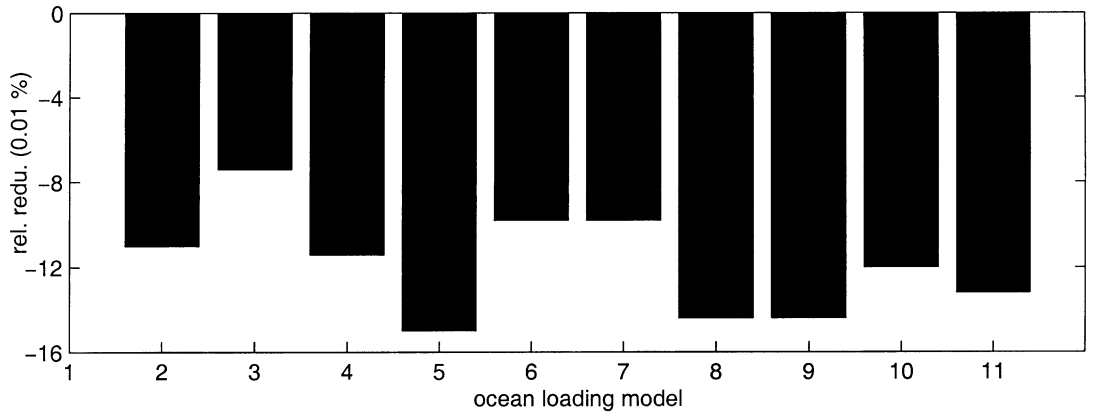

Fig. 10. Relative reduction (rel. redu.) in 0.01% of the χ^2 of the post-fit residuals by using different ocean loading models with respect to standard ocean loading using ocean loading based on the ocean tide model by Schwiderski (1980).

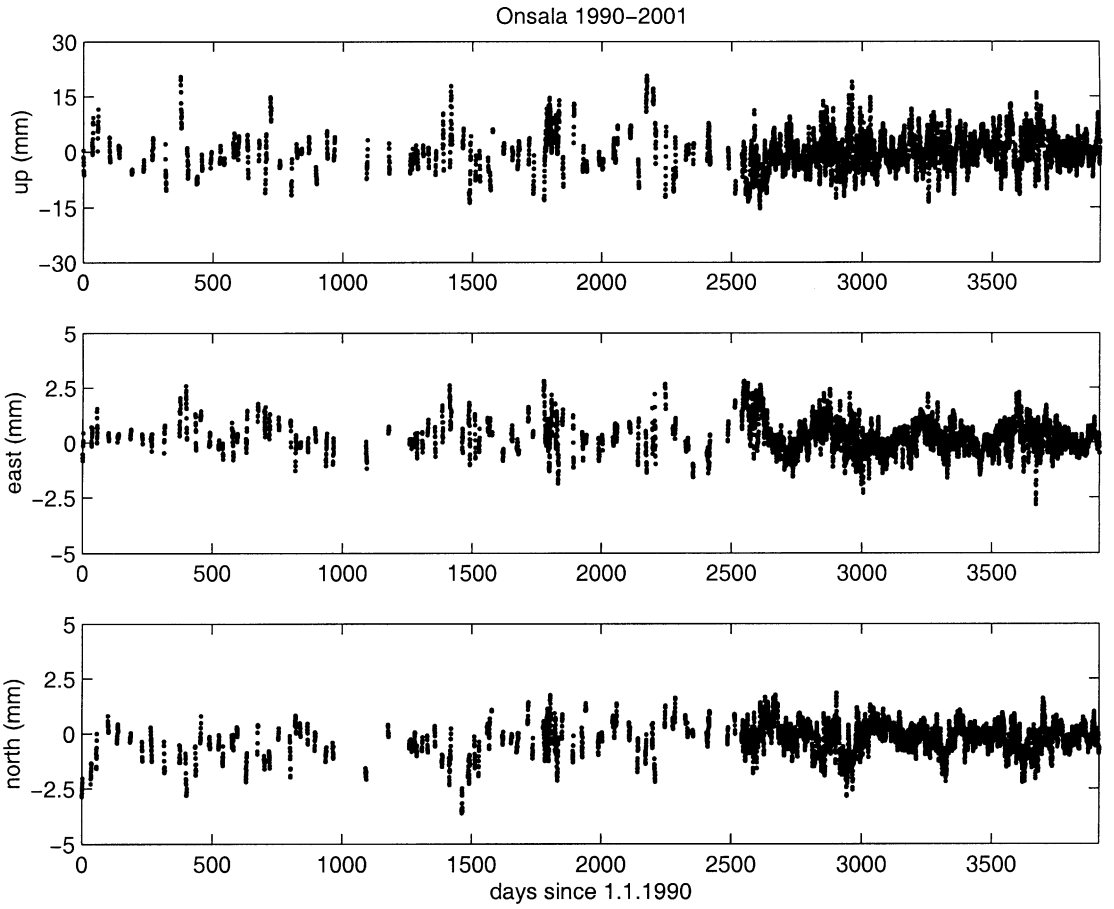

Fig. 11. Atmospheric loading effects at Onsala modeled by global convolution for the time period January 1990 to the end of December 2001.

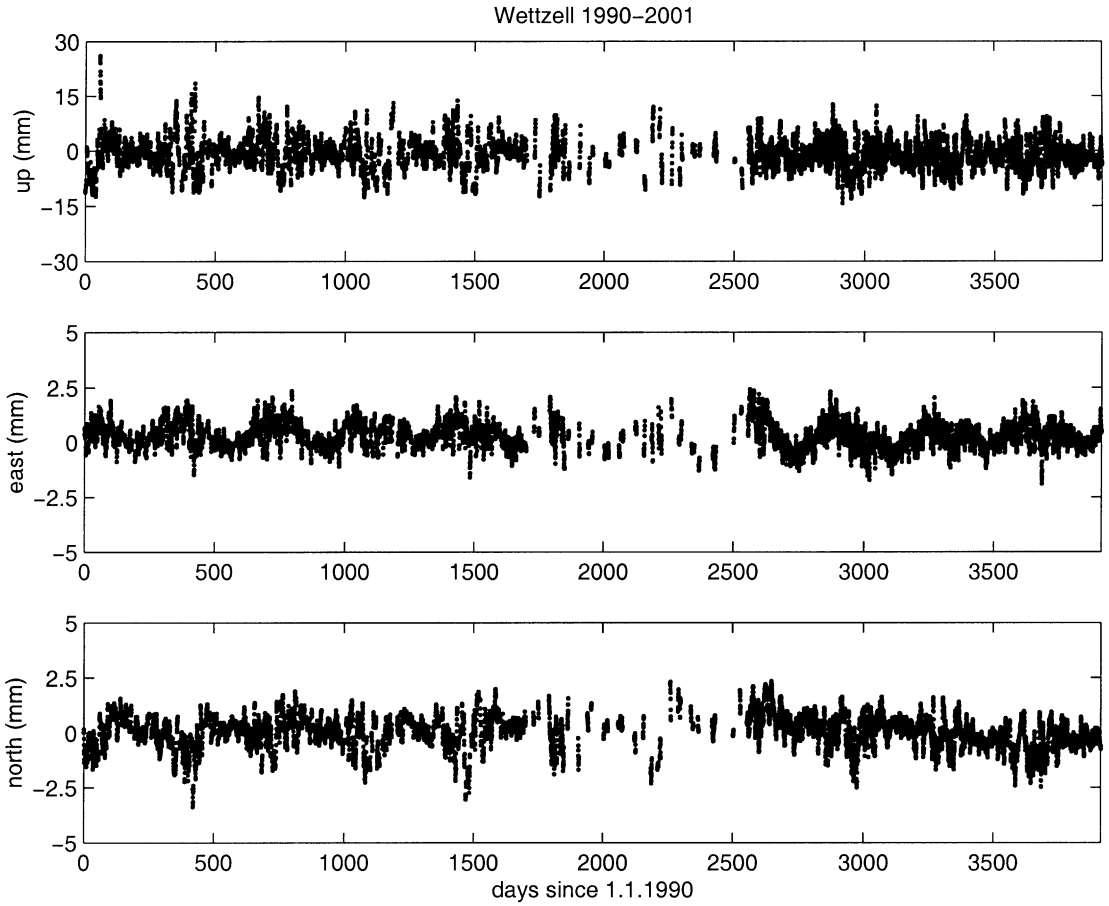

Fig. 12. Atmospheric loading effects at Wettzell modeled by global convolution for the time period January 1990 to the end of December 2001.

effects amount to up to 10 mm. The standard analysis software is extended to apply the atmospheric loading effects based on global convolution calculations for all European VLBI stations.

2.5. *Thermal deformation of the radio telescopes*

The radio telescopes are large mechanical constructions of concrete and metal. Thus, deformation effects of the telescopes and their reference points occur due to the thermal expansion of the constructions. A model for the thermal deformation effects based on the telescope dimensions, expansion coefficients and temperature readings at the sites has been developed (Nothnagel et al., 1995; Haas et al., 1998) and is applied in the data analysis. Actual monitoring of the vertical expansion of the telescopes at Onsala and Wettzell by invar measurement devices (Elgered and Carlsson, 1995; Kilger, 1996) can be used to calibrate this simple model. Fig. 14 shows vertical height variations monitored at the telescopes Onsala and Wettzell with the invar measurement devices (continuous lines) and the modelled values using the simple model (stars in circles).

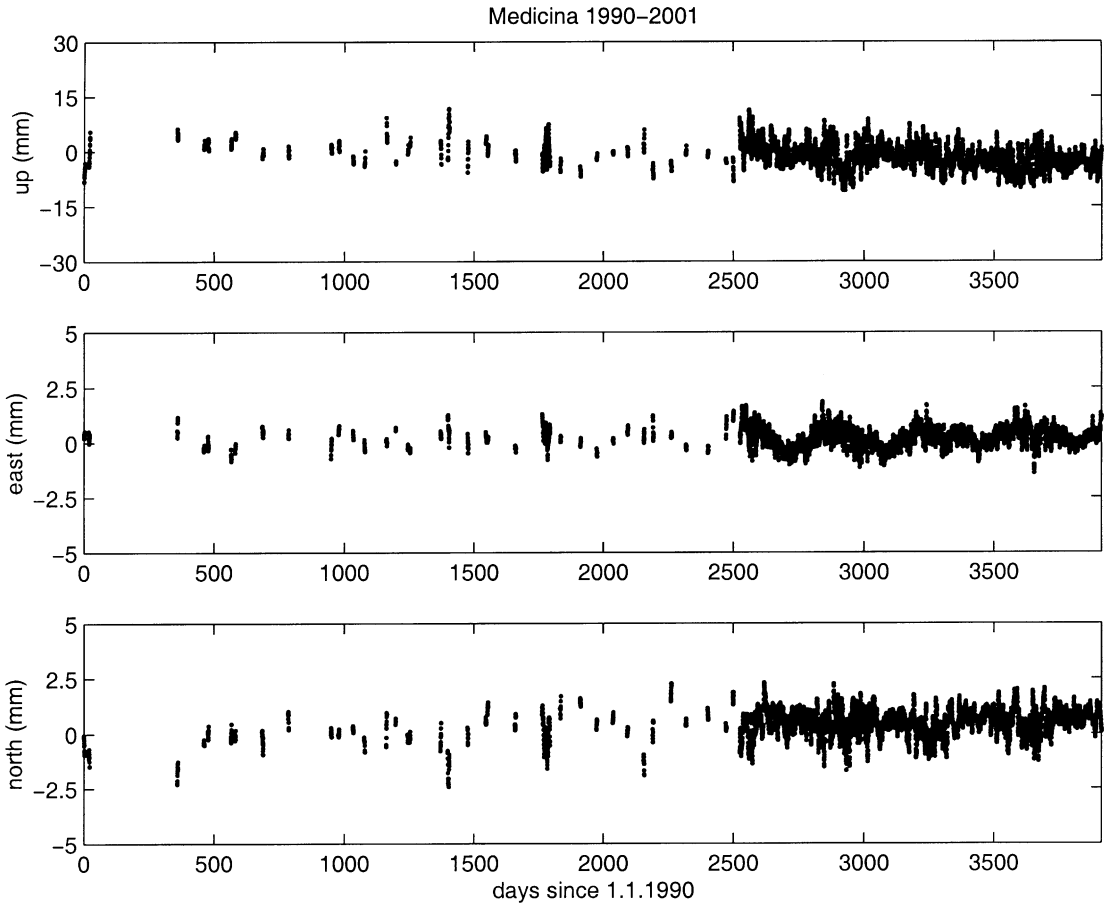

Fig. 13. Atmospheric loading effects at Medicina modeled by global convolution for the time period January 1990 to the end of December 2001.

2.6. Signal propagation in the atmosphere

The analysis of geodetic VLBI data has to take into account the variations in the radio refractive index in the atmosphere which manifest themselves as excess propagation delays. The main part of the atmospheric propagation delay is modelled based on the total ground pressure measured at the observing VLBI sites. In order to compensate for unmodelled atmospheric refraction effects, atmospheric zenith path delays are estimated every 60 min applying the NMF 2.0 mapping functions (Niell, 1996). All VLBI observations with minimum elevation of 5° above the local horizon are included in the analysis. Additionally, horizontal asymmetries in the atmospheric refraction profile are estimated in form of horizontal gradient parameters in north and east direction every 6 h. The gradients are modelled as described in Davis et al. (1993) and MacMillan (1995). Both types of atmospheric parameters, the zenith path delays and horizontal gradient parameters, are estimated as piece-wise linear functions. It has been shown by Herring et al. (1990) that random walk processes describe the variability of the wet delay reasonably well. Thus,

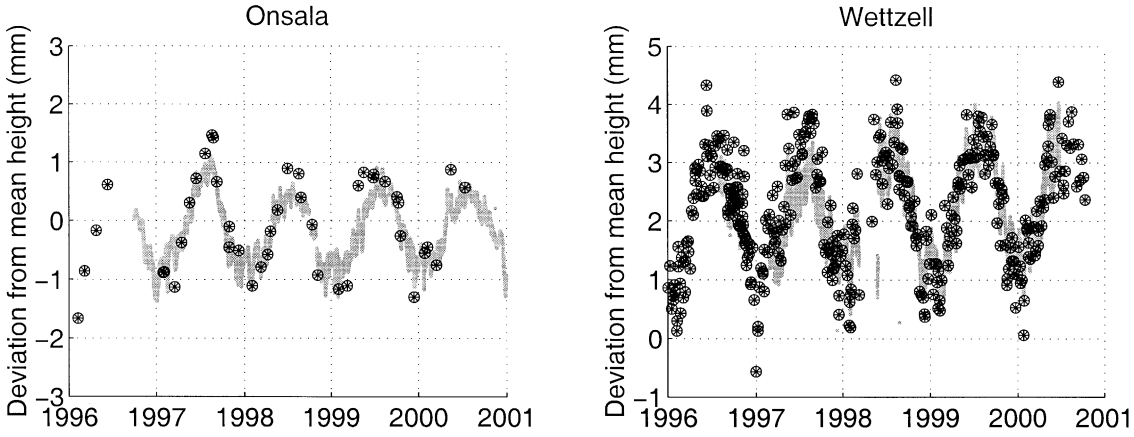

Fig. 14. Thermal deformation effects measured with invar measurement devices (solid lines) and modelled with a simple model for the stations Onsala and Wettzell (stars with circles).

the analysis software is improved to use linearly time dependent variances to form the constraints for the estimation of the atmospheric parameters.

Extensive comparisons of atmospheric parameters obtained from VLBI and independent techniques like the Global Positioning System (GPS), microwave radiometry (WVR), radiosondes and numerical weather models have been performed for several of the European VLBI sites (Gradinarsky al., 2000; Behrend et al., 2001). These investigations show positive correlation coefficients in the range of 0.8–0.9 for the zenith path delays and 0.3–0.6 for the horizontal gradient parameters.

3. Results for baseline measurements

The time series of geocentric station coordinates relative to the reference station are used to calculate baseline lengths and to analyse their evolution. Baseline lengths are invariant to rotational changes and thus give a good insight into the actual measurement accuracy. For each baseline, the mean baseline length, its rate and the corresponding weighted root-mean-square (wrms) scatter is calculated. For baselines including stations that suffered track and wheel repair, additional discontinuities at these epochs are estimated in the regression. Fig. 15 shows the temporal evolution of the baseline measurements on the nine baselines involving the reference station Wettzell, ordered in increasing baseline length. Given are also the baseline length rates and the weighted root-mean square scatter (wrms) values. The two baselines involving Simeiz and Yebes suffer from a short observation history, low number of observations and large scatter and thus indicate the low quality of the data recorded at these two stations. Both stations suffered of severe technical problems during the last years and unfortunately did not live up to the expectations yet.

Fig. 16 shows the corresponding spectra of the baseline length measurements calculated using the Lomb periodogram technique (Press et al., 1992) that allows the determination of spectra from unevenly sampled data. The purpose is to detect possible unmodelled periodic effects. The

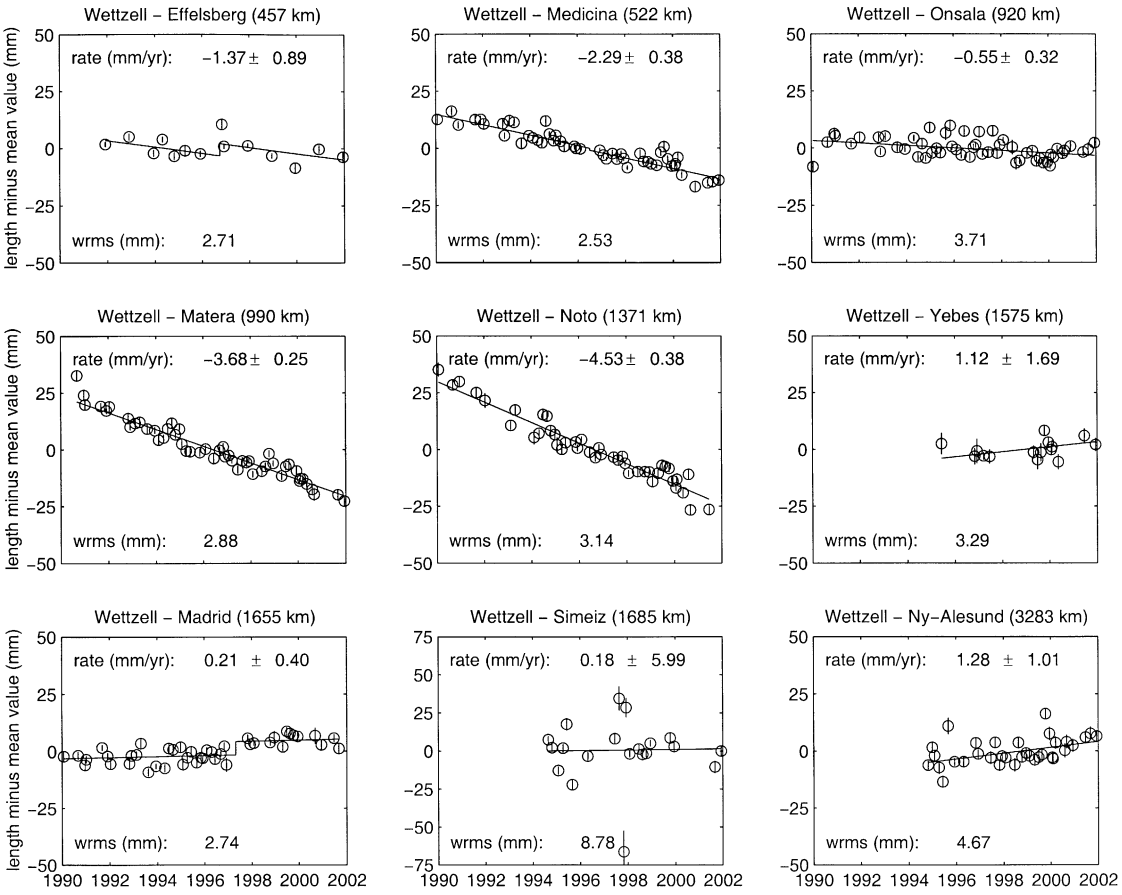

Fig. 15. Time series of baselines measurements involving Wettzell. Shown are the individual baseline measurements and the estimated regression lines.

vertical dashed lines indicate from right to left the frequencies corresponding to 1/2, 1, 2, 3 and 4 years. Some of the baselines show spectral energy close to the periods of 1/2 year and 1 year, e.g. the baselines to Medicina, Matera, Noto, Madrid and Ny-Ålesund. The two baselines involving Simeiz and Yebes do not show spectral energy at long periods. They show noise-like spectra, again indicating the poor performance of the baseline measurements involving these two stations.

Fig. 17 shows the weighted root-mean square scatter (wrms) of the individual baseline measurmenets with respect to the regression lines as a function of baseline length for all baselines except those involving the two stations Simeiz and Yebes. The relation between wrms and baseline length gives insight into the reproducability of the baseline measurements and thus into the precision of the baseline measurements. From a linear regression we see that the reproducability of the baseline measurements is as good as 2.0 mm plus an additional term depending on the baseline length of less than 1 part-per-billion (ppb). This shows that geodetic VLBI is one of the most precise space geodetic techniques to measure crustal movements.

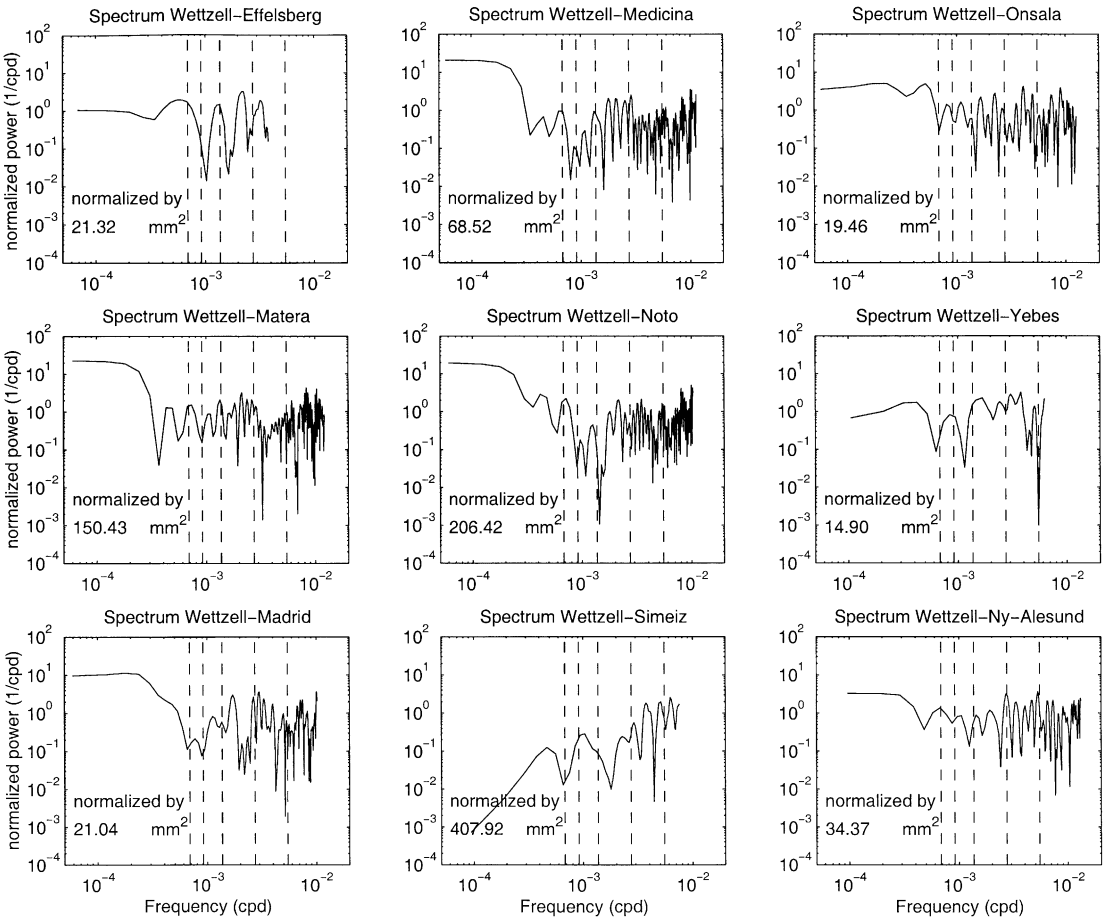

Fig. 16. Lomb periodogram spectra of the baselines measurements involving Wettzell. The frequencies corresponding to 1/2, 1, 2, 3, and 4 years are indicated from right to left with vertical dashed lines.

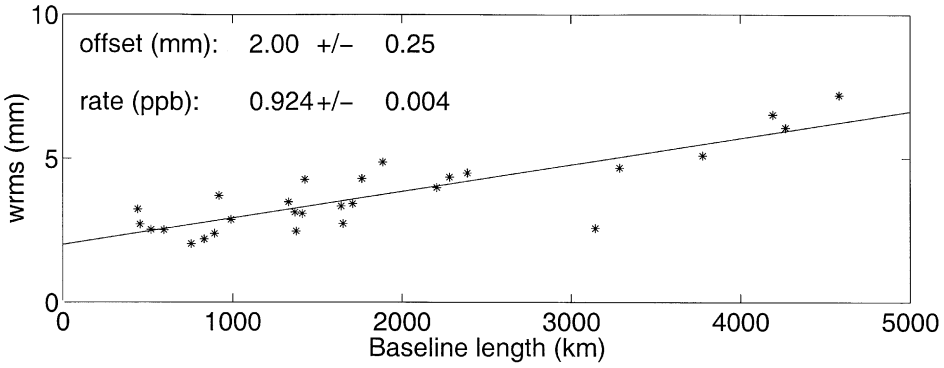

Fig. 17. Baseline measurement reproducability from analysis of the European geodetic VLBI data. Baselines involving Simeiz and/or Yebes are not shown.

4. Results for topocentric station motion

As described in Section 2, in a second step of the analysis the topocentric station motions are derived. Figs. 18–26 show time series of topocentric vertical and horizontal coordinates of the stations with respect to the reference station Wettzell and the corresponding spectra. The time series show the measurements together with their error bars and the estimated regression lines. For Medicina, Effelsberg and Madrid the estimated site displacements due to track and wheel repairs are shown as jumps in the regression lines and for those station where annual amplitudes proved to be statistically significant from hypothesis tests the annual signatures are shown too.

The estimated vertical 'jump' of Effelsberg of $+20.7\pm15.1$ mm agrees well with the result of a local survey of $+21.8\pm1.0$ mm (Nothnagel, 1999). For Medicina the estimated vertical 'jump' of $+13.8\pm8.5$ mm agrees within its formal error with the result from a local survey of $+18.5\pm2.1$

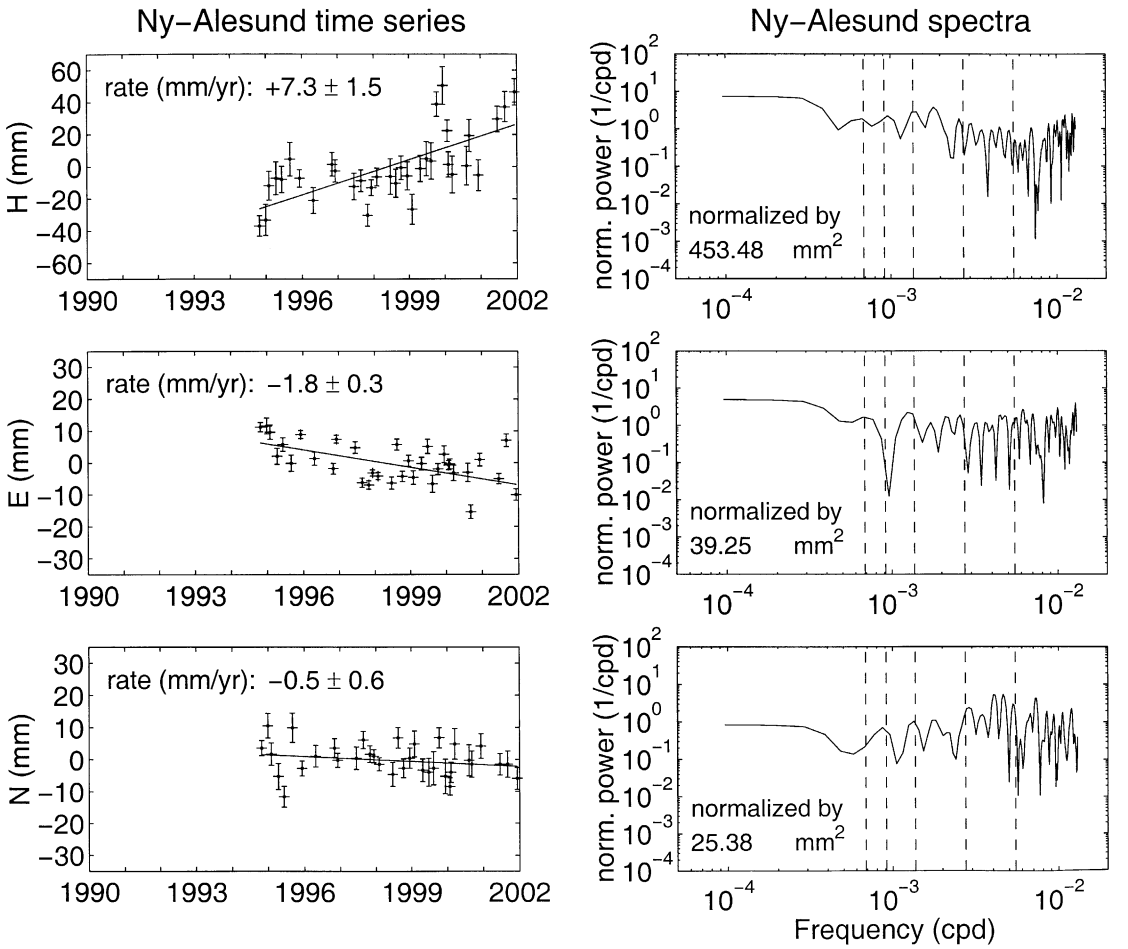

Fig. 18. Time series of topocentric coordinates of Ny-Ålesund with respect to Wettzell (left column) and the corresponding Lomb periodogram spectra (right column). The frequencies corresponding to 1/2, 1, 2, 3, and 4 years are indicated from right to left with vertical dashed lines.

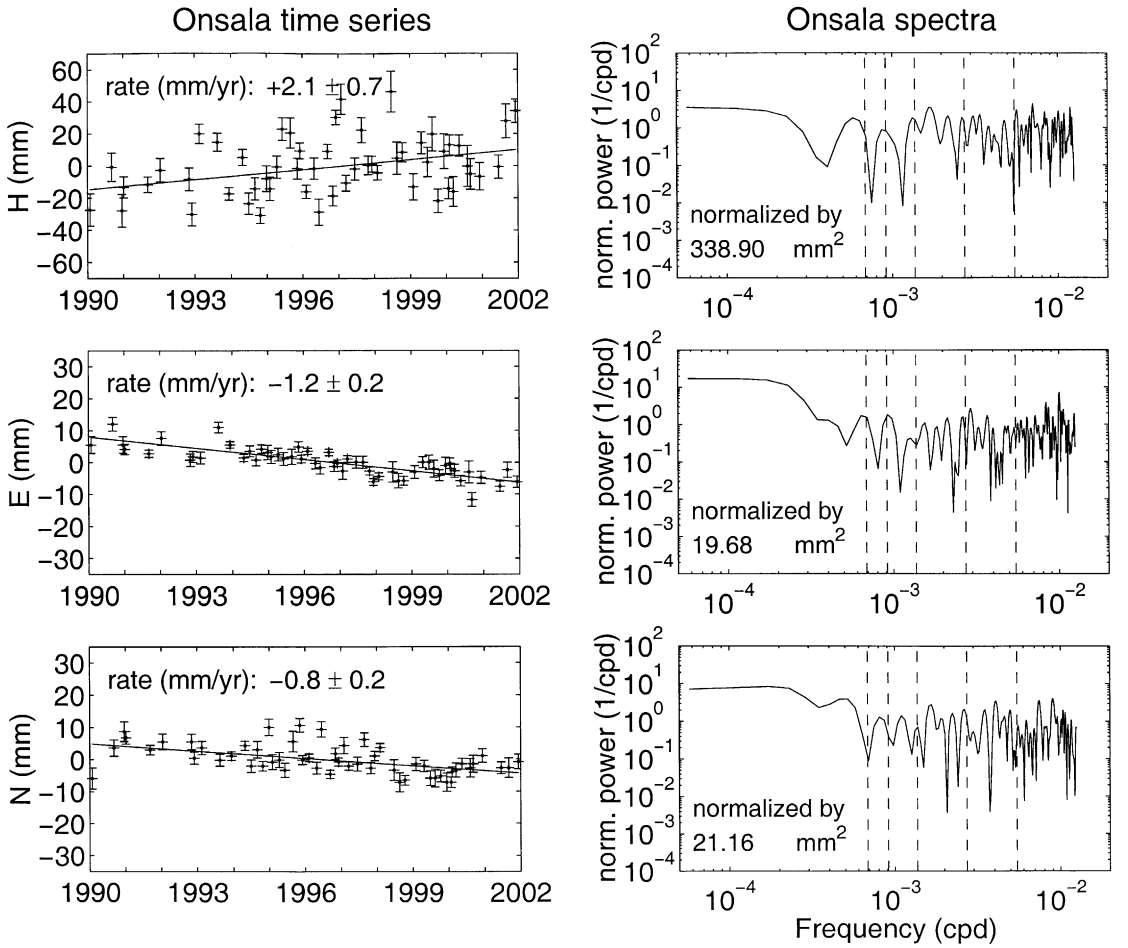

Fig. 19. Time series of topocentric coordinates of Onsala with respect to Wettzell (left column) and the corresponding Lomb periodogram spectra (right column). For explanation see caption of Fig. 18.

mm (Nothnagel and Binnenbruck, 2000). However, the estimated 'jumps' in east and north component of -3.3 ± 2.1 mm and $+2.0\pm2.4$ mm, respectively, do not agree with the results of a local survey of $+4.0\pm2.8$ mm and -2.6 ± 2.8 mm (Nothnagel and Binnenbruck, 2000). At Madrid the estimated 'jump' of -12.9 ± 3.1 mm in the north component appears to be significant and corresponds at least in direction with the result of a local survey of -7.0 ± 3.8 mm (Behrend, 1998).

Note that the up-component of Yebes in the first session shows a large deviation that forced us to introduce a 'jump' without knowing the actual reason for it. Note also that there are two sessions where the up-components of Simeiz lie outside the drawing area and only parts of the errorbars become visible. These results stress again the poor performance of these two stations.

The spectra are again calculated as Lomb periodograms and the frequencies corresponding to 1/2, 1, 2, 3, and 4 years are indicated from right to left with vertical dashed lines. The spectra for Effelsberg show some spectral energy close to a period of 1 year in particular for the up-component. This is probably an artefact due to the sampling of the observation sessions involving

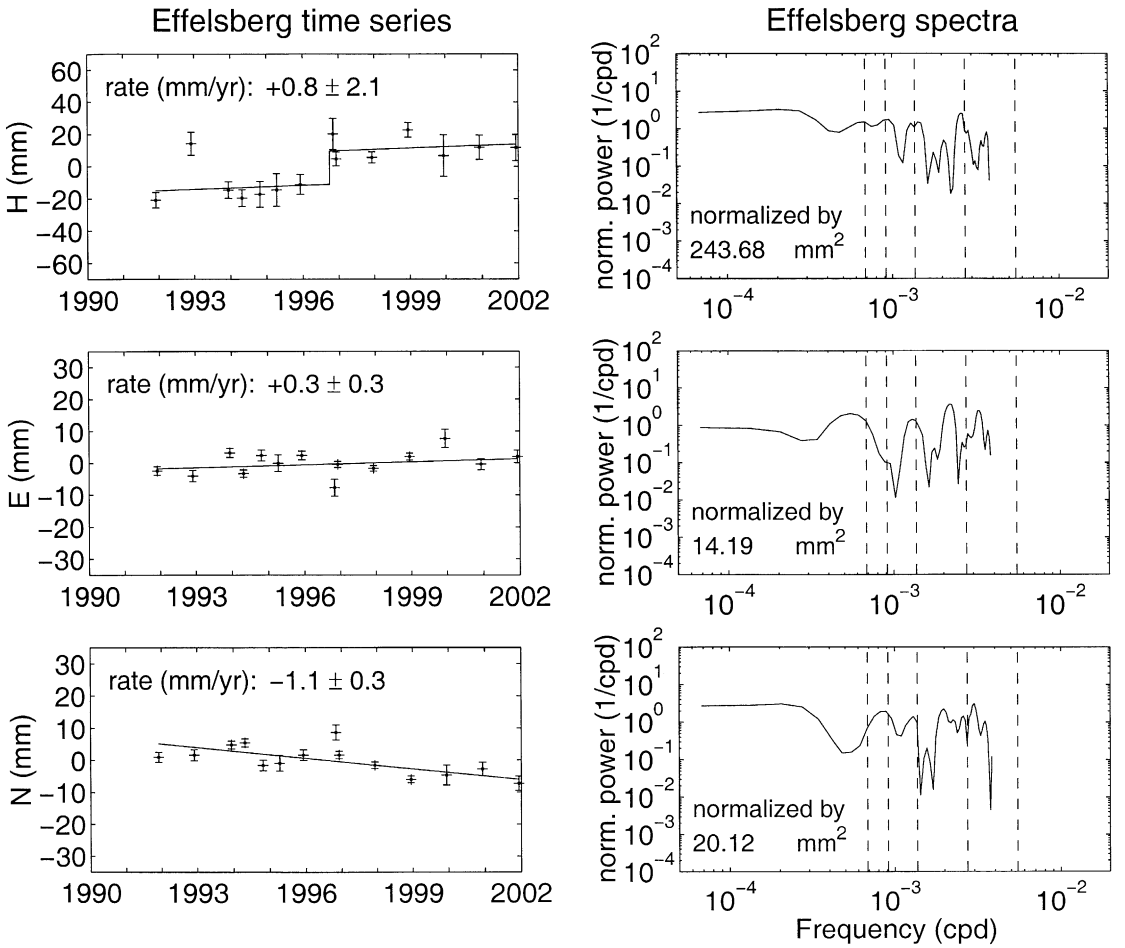

Fig. 20. Time series of topocentric coordinates of Effelsberg with respect to Wettzell (left column) and the corresponding Lomb periodogram spectra (right column). For explanation see caption of Fig. 18.

Effelsberg, because this radio telescope is unfortunately only available once per year for geodetic VLBI. The estimated annual signal is not statistically significant. The Madrid spectra reveal spectral energy close to a period of 1 year and 2 years for the up-component and some spectral energy close to a period of 1 year for the north component. The estimation of an annual signal proves only to be statistically significant for the up-component. Since thermal deformation effects of the telescopes with a clear annual signature are considered already in the VLBI analysis, these annual signals are probably due to other environmental influences, e.g. water table variations. The Yebes spectra appear to be noise-like without clear features and manifest the unfortunately poor data quality. Medicina's spectra show some spectral energy close to the annual and bi-annual periods for the up-component and close to the annual period for the horizontal components. The estimation of annual signals appears to be statistically significant for the up- and the north-component. The reasons for these annual signals could again be environmental influences, e.g. water table variations in the Po valley close to the Medicina site. Also the spectra of Matera

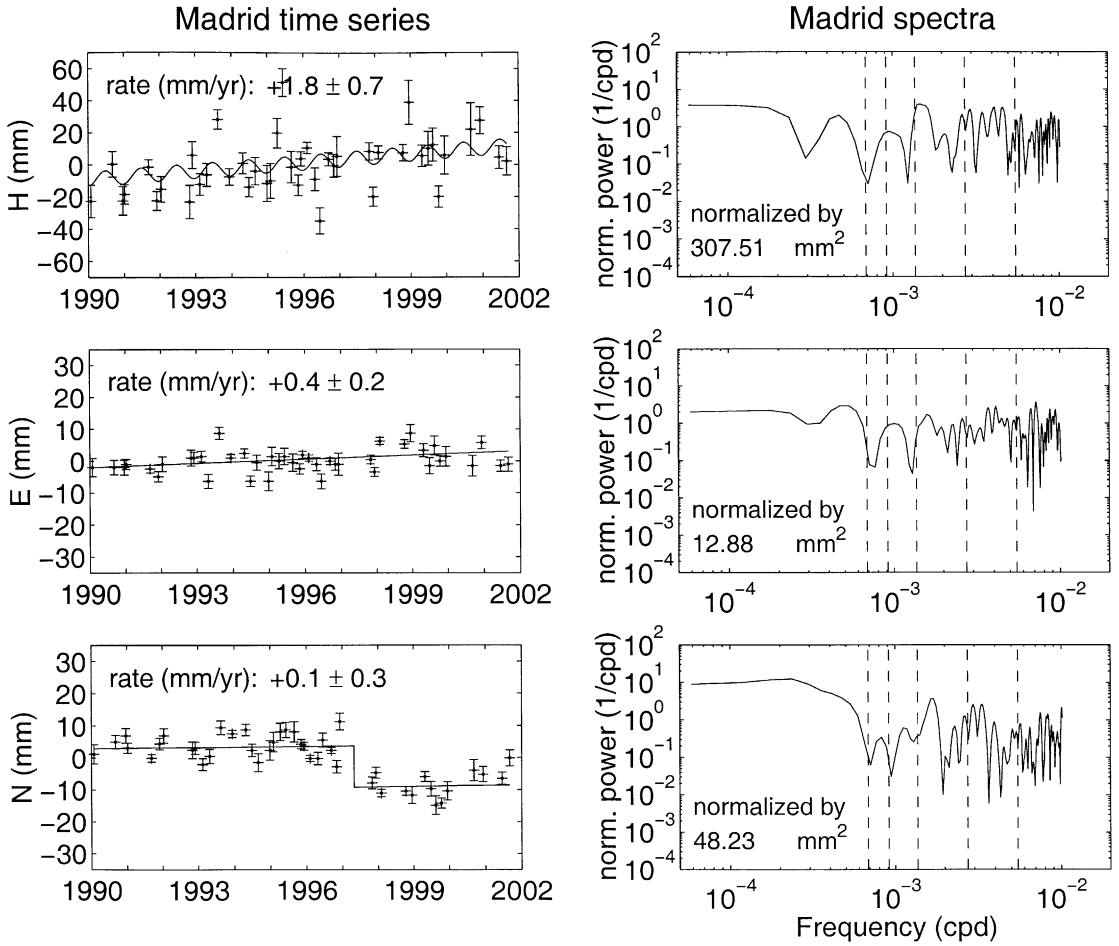

Fig. 21. Time series of topocentric coordinates of Madrid with respect to Wettzell (left column) and the corresponding Lomb periodogram spectra (right column). For explanation see caption of Fig. 18.

reveal some spectral energy close to the annual period, and for the up-component also for the bi-annual period. Statistically significant annual signals are estimated for the up- and the north-component. Also here the reasons are probably of environmental origin. The spectra for Noto show only some spectral energy in the vicinity of the semi-annual and annual periods for the up-component. The estimation of an annual signal is statistically significant. The Simeiz spectra appear to be similar to the Yebes spectra, i.e. noise-like without clear features.

Table 2 summarises the results for topocentric movements and weighted root-mean square scatter. With the exception of Simeiz and Yebes, the horizontal velocities have formal errors in the range of 0.2–0.7 mm/year and the vertical velocities have formal errors in the range of 0.6–2.6 mm/year. Thus, significant horizontal crustal movements are determined with relative accuracies in the range of 10–40%, significant vertical crustal movements are determined with relative accuracies in the range of 30–40%.

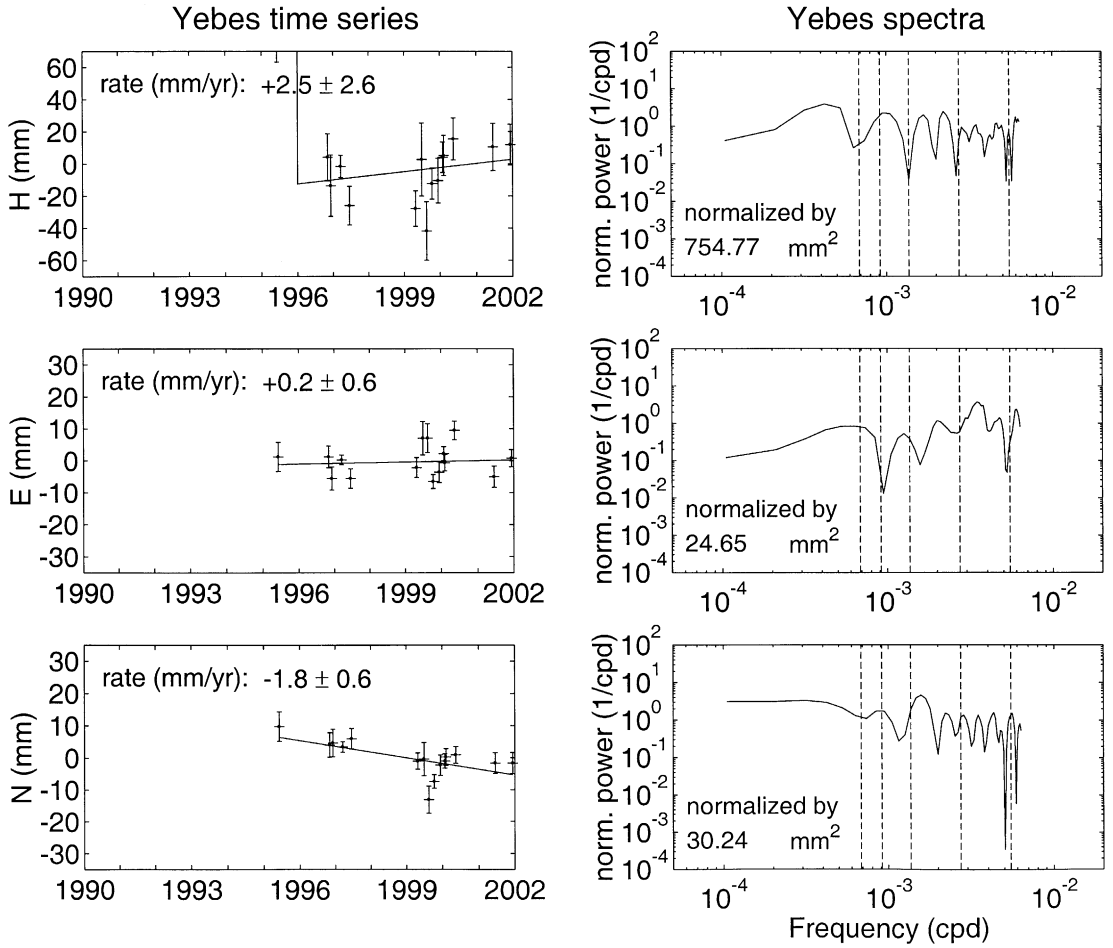

Fig. 22. Time series of topocentric coordinates of Yebes with respect to Wettzell (left column) and the corresponding Lomb periodogram spectra (right column). For explanation see caption of Fig. 18.

Table 2
Horizontal and vertical velocities with respect to Wettzell and the corresponding weighted root-mean square scatter (wrms)

Station	East rate (mm/year)	wrms (mm)	North rate (mm/year)	wrms (mm)	Vertical rate (mm/year)	wrms (mm)
Effelsberg	+0.3±0.3	2.5	−1.1±0.3	2.9	+0.8±2.1	8.6
Madrid	+0.4±0.2	3.1	+0.1±0.3	3.4	+1.8±0.7	13.5
Matera	+1.7±0.2	2.5	+4.2±0.2	2.7	+0.0±0.6	14.7
Medicina	+2.1±0.2	2.0	+1.8±0.2	2.4	−3.0±0.8	7.8
Noto	−0.1±0.2	3.1	+4.5±0.2	3.3	−0.4±0.7	9.5
Ny-Ålesund	−1.8±0.3	5.1	−0.5±0.6	4.5	+7.3±1.5	14.3
Onsala	−1.2±0.2	2.6	−0.8±0.2	3.4	+2.1±0.7	15.9
Simeiz	+0.6±0.8	7.5	+1.7±0.9	3.2	+1.5±3.5	38.8

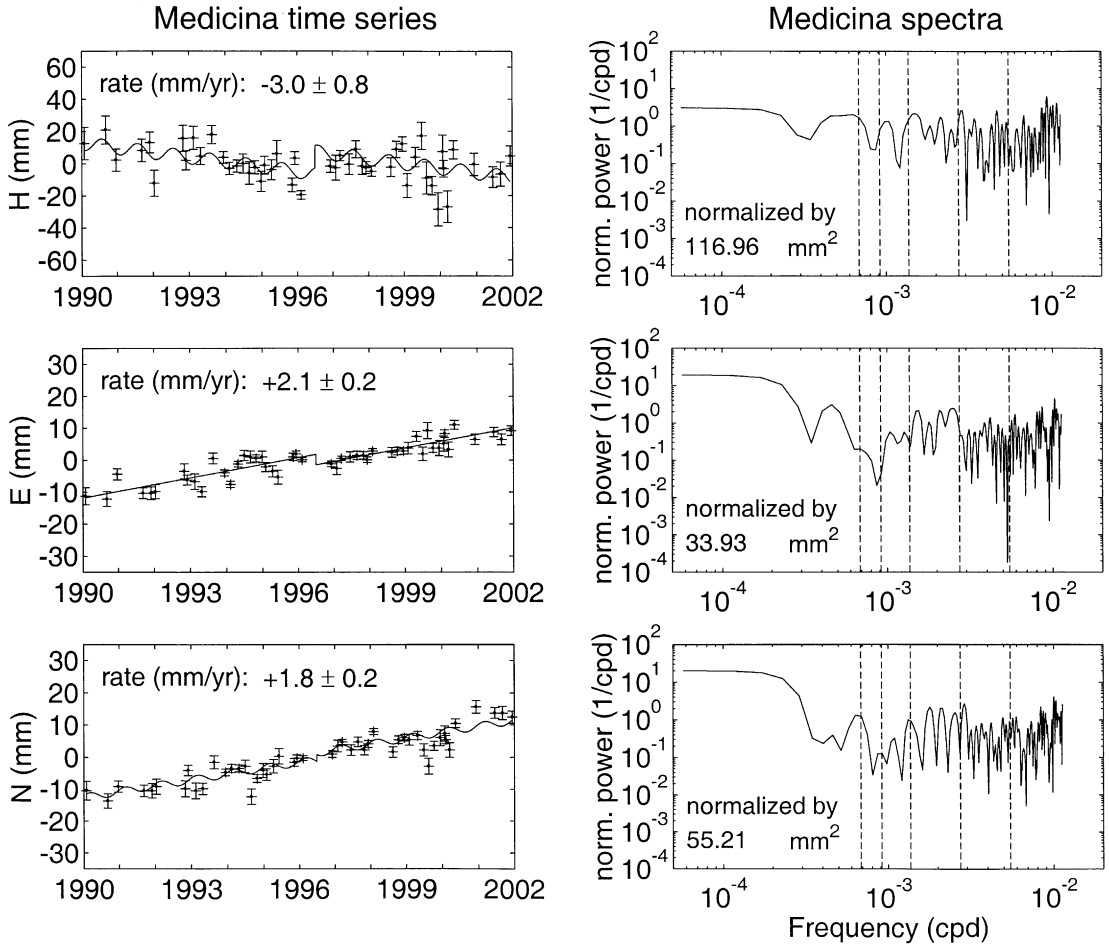

Fig. 23. Time series of topocentric coordinates of Medicina with respect to Wettzell (left column) and the corresponding Lomb periodogram spectra (right column). For explanation see caption of Fig. 18.

5. Discussion and outlook

With nearly 60 observation sessions in 12 years the European geodetic VLBI network allows the determination of crustal movements in Europe with high accuracy. Baseline measurements are possible with an accuracy of 2.0 mm plus an additional baseline dependent term of less than 1 ppb. Horizontal motions significantly different from zero are determined with relative accuracies in the range of 10–40%, vertical crustal movements significantly different from zero are determined with relative accuracies in the range of 30–40%, respectively. The chi-square values of the position residuals are in the range of 2.5–6 for the stations with sufficient observation history.

The Italian stations Noto, Matera and Medicina show north directed and north-east directed horizontal motion with respect to Wettzell. While Noto is moving by 4.5 mm/year with azimuth

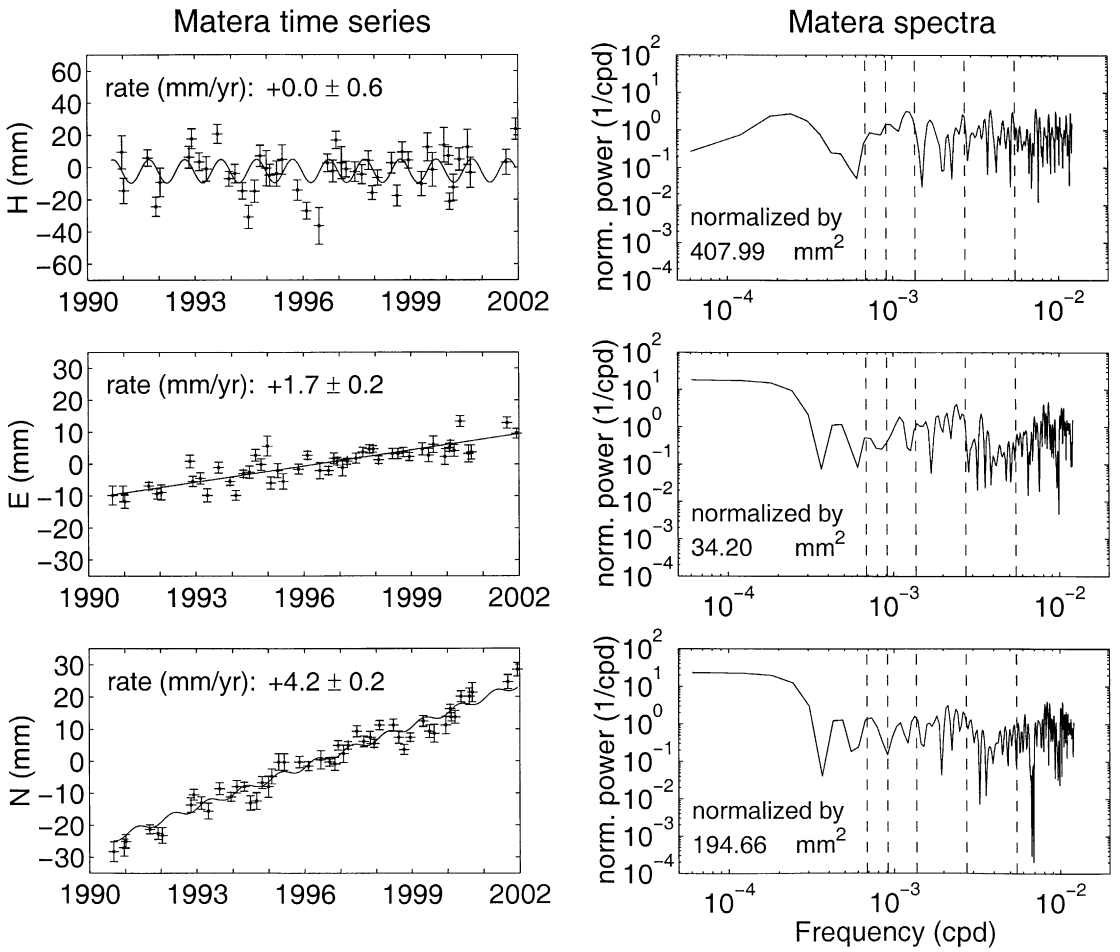

Fig. 24. Time series of topocentric coordinates of Matera with respect to Wettzell (left column) and the corresponding Lomb periodogram spectra (right column). For explanation see caption of Fig. 18.

359°, Matera moves by 4.5 mm/year with azimuth 22°, and Medicina has a motion of 2.8 mm/year with azimuth 49°. Noto and Matera do not show a significant vertical motion while Medicina appears to subside by 3.0 mm/year.

Madrid appears to move horizontally by 0.4 mm/year with azimuth 75° with respect to Wettzell. The station shows a vertical motion relative to Wettzell of 1.8 mm/year. The results for the other Spanish station Yebes cannot be taken as significant yet. The result for horizontal motion of Simeiz with respect to Wettzell of 1.8 mm/year with azimuth 19° has to be interpreted very carefully. The vertical motion of Simeiz is not significant.

Effelsberg appears to move horizontally by 1.1 mm/year with azimuth 165° with respect to Wettzell. The station does not reveal a significant vertical motion. For Effelsberg, the low number of observation sessions involving the station is the largest obstacle for the determination of results with a higher level of significance.

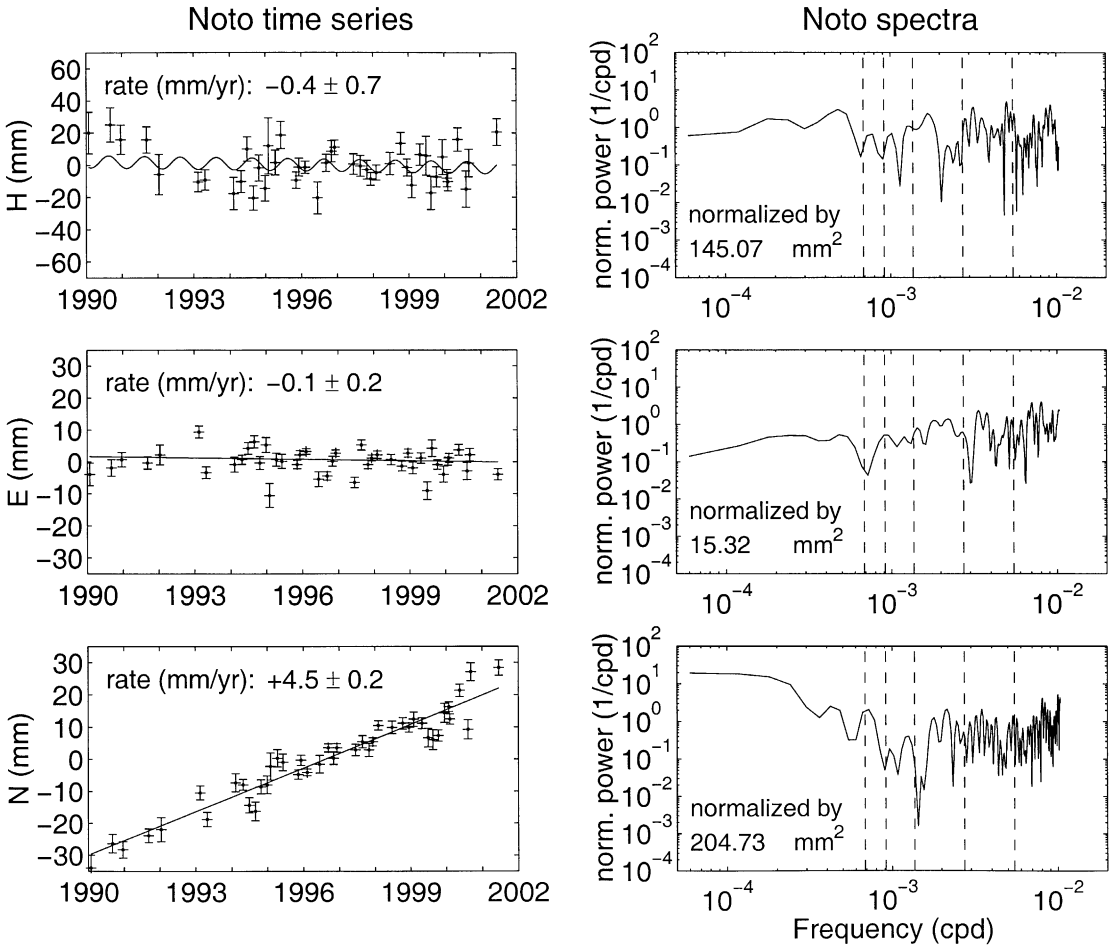

Fig. 25. Time series of topocentric coordinates of Noto with respect to Wettzell (left column) and the corresponding Lomb periodogram spectra (right column). For explanation see caption of Fig. 18.

The two northern stations Onsala and Ny-Ålesund show significant motion with respect to Wettzell. Onsala shows a horizontal movement of 1.4 mm/year with azimuth 236° and a vertical motion of 2.1 mm/year. Ny-Ålesund appears to move horizontally by 1.9 mm/year with azimuth 254° and shows a large vertical uplift by 7.3 mm/year.

Some of the stations also reveal statistically significant annual variations especially for their up- and north-components. These variations probably can be related to environmental influences like annual water table variations.

The derived horizontal and vertical crustal movements yield a sound basis for interpretations in a geophysical and geological context. However, the data quality of the stations with a short observing history does not live up to the expectations yet and the crustal motion results for these stations do not yet reach the quality and confidence of the other stations.

For the future a densification of the European geodetic VLBI network is desired. Several radio telescopes that are under construction or are in a process of upgrade right now will be included in

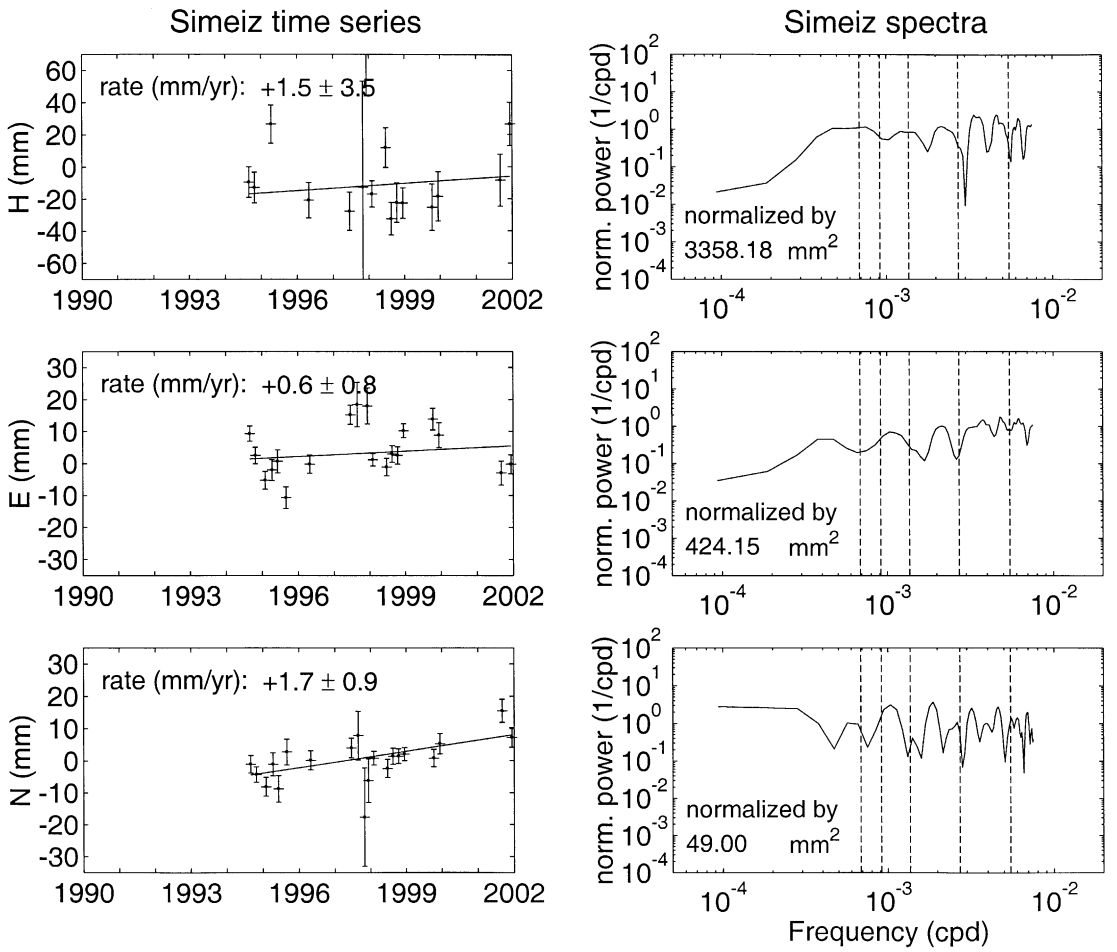

Fig. 26. Time series of topocentric coordinates of Simeiz with respect to Wettzell and the corresponding Lomb periodogram spectra (right column). For explanation see caption of Fig. 18.

the observation sessions in the near future. Also a combination with more densly distributed space geodetic techniques, in particular GPS, is a promising approach for future investigations.

References

Behrend, D., 1998. Invariant Point I, Geodetic Determination of the Invariant Point of the DSS65 VLBI Antenna (Technical Report 98-01). Evaluation of Four IGN Measurement Campaigns. Institut d'Estudis Espacials de Catalunya, Consejo Superior de Investigationes Científicas, Barcelona, Spain.

Behrend, D., Haas, R., Pino, D., Gradinarsky, L.P., Keihm, S.J., Schwarz, W., Cucurull, L., Rius, A., 2001. MM5 derived ZWDs compared to observational results from VLBI, GPS and WVR. Phys. Chem. Earth 27, 301–308.

Campbell, J., 1995. Managing Geodetic VLBI in Europe: The European Crustal Motion Network. In: Lanotte, R., Bianco, G. (Eds.), Proc. of the 10th Working Meeting on European VLBI for Geodesy and Astrometry. Matera, Italy, pp. 79–86.

Campbell, J., 1996. Measurement of Vertical Motion in Europe by VLBI—Further Support of the European Geodetic VLBI network by the European Union. In: Elgered, G. (Ed.), Proc. of the 11th Working Meeting on European VLBI for Geodesy and Astrometry. Onsala, Sweden, pp. 227–231.

Campbell, J., 1997. Measurement of Vertical Motion in Europe by VLBI—Status of the EU-TMR Network. In: Pettersen, B.-R. (Ed.), Proc. of the 12th Working Meeting on European VLBI for Geodesy and Astrometry. Norway, Hønefoss, pp. 1–8.

Campbell, J., Nothnagel, A., 2000. European VLBI for crustal dynamics. Journal of Geodynamics 30, 321–326.

Davis, J.L., Elgered, G., Niell, A.E., Kuehn, C.E., 1993. Ground-based measurements of gradients in the "wet" radio refractivity of air. Radio Science 28 (6), 1003–1018.

De Mets, C., Gordon, R.G., Argus, D.F., Stein, S., 1994. Effect of recent revision to the geomagnetic reversal time scale on estimates of current plate motions. Geophys. Res. Lett. 21 (20), 2191–2194.

Eanes, R.J., Bettadpur, S., 1995. The CSR 3.0 global ocean tide model. Technical Memorandum CSR-TM-95-06. Center for Space Research, University of Texas, Austin, TX.

Egbert, G.D., Bennett, A.F., Foreman, M.G.G., 1994. TOPEX/POSEIDON tides estimated using a global inverse model. J. Geophys. Res. 99, 24821–24852.

Elgered, G., Carlsson, T.R., 1995. Temperature Stability of the Onsala 20-m Antenna and its Impact on Geodetic VLBI. In: Lanotte, R., Bianco, G. (Eds.), Proc. of the 10th Working Meeting on European VLBI for Geodesy and Astrometry. Matera, Italy, pp. 69–78.

Farrel, W.E., 1972. Deformation of the Earth by surface loads. Rev. Geophys. Space Phys. 10 (3), 761–797.

Gradinarsky, L.P., Haas, R., Elgered, G., Johansson, J.M., 2000. Wet path delay and delay gradients observed with microwave radiometry, VLBI, and GPS. Earth Planets Space 52, 695–698.

Gueguen, E., Doglioni, C., Fernandez, M., 1998. On the post-25 Ma geodynamic evolution of the western Mediterranean. Tectonophysics 298, 259–269.

Haas, R., Nothnagel, A., Schuh, H., Titov, O., 1998. Explanatory Supplement to the Section 'Antenna Deformation' of the IERS Conventions (1996). In: H. Schuh (Ed.), DGFI Report, 71, Deutsches Geodätisches Forschungsinstitut (DGFI), pp. 26–29.

Haas, R., Nothnagel, A., 1999. A two-step approach to analyze European geodetic Very Long Baseline Interferometry (VLBI) data. In: Schlüter, W., Hase, H. (Eds.), Proc. of the 13th Working Meeting on European VLBI for Geodesy and Astrometry. Bundesamt für Kartographie und Geodäsie, Wettzell, 108–114.

Haas, R., Gueguen, E., Scherneck, H.G., Nothnagel, A., Campbell, J., 2000. Crustal motion results derived from observations in the European geodetic VLBI network. Earth Planets Space 52, 759–764.

Herring, T.A., Davis, J.L., Shapiro, I.I., 1990. Geodesy by radio interferometry: the application of kalman filtering to the analysis of Very Long Baseline Interferometry data. Journal of Geophysical Research 95, 12561–12581.

International Earth Rotation Service (IERS), 2000. IERS Earth Orientation Parameters Product Center. Available: http://hpiers.obspm.fr/eop-pc/.

Kilger, R., 1996. Status report of RT-Wettzell. In: Elgered, G. (Ed.), Proc. of the 11th Working Meeting on European VLBI for Geodesy and Astrometry. Onsala, Sweden, pp. 18–20.

Le Provost, C., Genco, M.L., Lyard, F., Vincent, P., Canceil, P., 1994. Spectroscopy of the world ocean tides from a finite element hydrological model. J. Geophys. Res. 99, 24777–24798.

Le Provost, C., Lyard, F., Molines, J.M., Genco, M.L., Rabilloud, F., 1998. A hydrodynamic ocean tide model improved by assimilating a satellite altimeter-derived data set. J. Geophys. Res. 103 (C3), 5513–5529.

Lefèvre, F., Lyard, F.H., Le Provost, C., 2000. FES99: a new global tide finite element solution independent of altimetry. Geophys. Res. Letters 27, 2717–2720.

Lieske, J.H., Lederle, T., Fricke, W., Morando, B., 1977. Expressions for the precession quantities based upon the IAU (1976) system of astronomical constants. Astron. Astrophys. 58, 1–16.

Ma, C., Sauber, J.M., Bell, L.J., Clark, T.A., Gordon, D., Himwich, W.E., Ryan, J.W., 1990. Measurement of horizontal motions in Alaska using very long baseline interferometry. J. Geophys. Res. 95 (2), 1991–22011.

Ma, C., Ryan, J.W., 1998. NASA Space Geodesy Program—GSFC Data Analysis—1998, VLBI Geodetic Results 1979–1998, August, 1998. Available: http://lupus.gsfc.nasa.gov/global/glb.html.

MacMillan, D.S., 1995. Atmospheric gradients from very long baseline interferometry observations. Geophysical Research Letters 22, 1041–1044.

Matsumoto, K., Takanezawa, T., Ooe, M., 2000. Ocean Tide Models Developed by assimilating TOPEX/POSEIDON altimeter data into hydrodynamical model: a global model and a regional model around Japan. J. Oceanog. 56, 567–581.

McCarthy, D.D. (Ed.), 1996. IERS Conventions (1996), IERS Technical Note 21. Observatoire de Paris.

Nothnagel, A., Pilhatsch, M., Haas, R., 1995. Investigations of thermal height chances of geodetic VLBI radio telescopes. In: Lanotte, R., Bianco, G. (Eds.), Proc. of the 10th Working Meeting on European VLBI for Geodesy and Astrometry. Agenzia Spatiale Italiana, pp. 121–133.

Nothnagel, A., 1999. Conventional Survey at the Effelsberg radio telescope—Internal Report 1999. Geodetic Institute Report. Available: http://giub.geod.uni-bonn.de. Geodetic Institute of the University of Bonn, 1999.

Nothnagel, A., Binnenbruck, B., 2000. Determination of the 1996 displacement of the Medicina radio telescope by local surveys. In: Tomasi, P., Mantovani, F., Perez-Torres, M.A. (Eds.), Proc. of the 14th Working Meeting on European VLBI for Geodesy and Astrometry. Consiglio Nazionale delle Ricerche, Instituto di Radioastronomia, Bologna, Italy, pp. 61–66.

Niell, A.E., 1996. Global mapping functions for the atmosphere delay at radio wavelength. J. Geophys. Res. 101, 3227–3246.

Press, W.H., Teukolsky, S.A., Vetterling, W.T., Flannery, B.P. (Eds.), 1992. Numerical Recipes in Fortran. second ed. Cambridge University Press, Cambridge.

Ray, R., 1999. A global ocean tide model from Topex/Poseidon altimetry: GOT99.2, 1999. NASA technical memorandum, NASA/TM-1999-209478. National Aeronautics and Space Administration, Goddard Space Flight Center, Greenbelt, MD.

Scherneck, H.G., 1991. A parametrized solid earth tide model and ocean loading effects for global geodetic baseline measurements. Geophys. J. Int. 106, 677–694.

Scherneck, H.G., Bos, M.S., 2001. An Automated Internet Service for Ocean Tide Loading Calculation. Available: http://www.oso.chalmers.se∼loading.

Schwiderski, E.W., 1980. On charting global ocean tides. Rev. Geophys. Space Phys. 18, 243–268.

Seidelmann, P.K., 1982. 1980 IAU Nutation: The Final report of the IAU Working Group on Nutation. Celest. Mech. 27, 79–106.

Sovers, O.J., Fanselow, J.L., Jacobs, C.S., 1998. Astrometry and geodesy with radio interferometry: experiments, models, results. Rev. Mod. Phys. 79 (4), 1393–1454.

Tamura, Y., 1997. A harmonic development of the tide-generating potential. Bulletin d'Information Marées Terrestres. 99, 6813–6855.

Wahr, J.M., 1981. Body tides on an elliptical, rotating, elastic and oceanless earth. Geophys. J. R. A. S. 64, 677–703.

Ward, S.N., 1994. Constraints on the seismotectonics of the central Mediterranean from Very Long Baseline Interferometry. Geophys. J. Int. 117, 441–452.